A nonlinear time series analysis on the effect of foot injury on gait dynamics

MIHAI DUPAC[1], DAN B. MARGHITU[2]
[1]Department of Design and Engineering,
Bournemouth University,
Talbot Campus, Fern Barrow, BH12 5BB, Poole, Dorset,
UK
[2]Department of Mechanical Engineering,
Auburn University,
1418 Wiggins Hall, Auburn, AL 36849,
USA

Abstract: - The effects of foot injuries regarding bilateral asymmetry and gait dynamics are still poorly understood. Previous work discussed rehabilitation, postural control, and asymmetry, with the models being mainly validated for upper body translations and no or minimal assessment on rotation. The aim of this study was to assess the effect of foot injury on gait dynamics. For this, a wearable sensors system for data collection of the key variables of the of human movement was considered. The dynamics of motion – recorded in the plane of motion using a laser sensor – was assessed using a new projective method which considers the axial rotations, translation, and in-plane rotation patterns for normal human gait vs. simulated gait pathologies. A nonlinear timeseries analysis, along with a Poincare map, phase space, time delay, Lyapunov exponents, and false nearest neighbors (FNN) method have been considered in order to convey the periodicity of the data collected for a healthy individual with and without a simulated injury. The Lyapunov exponents which quantity the degree of separation of nearby trajectories are used to differentiate between the chaotic and non-chaotic behavior. The positive sign of the largest Lyapunov exponents for all data indicated "the exponential separation of nearby trajectories as time evolves", that is, the chaotic behavior of the system.

Key-Words: - Nonlinear analysis, Lyapunov exponents, Poincare map, gait dynamics, wearable sensors

Received: March 15, 2024. Revised: October 17, 2024. Accepted: November 13, 2024. Published: December 11, 2024.

1 Introduction

The use of wearable sensors [1,2] and motion capture having reflective markers [3] has proved to be viable solutions in the dynamic analysis of gait and postural control. Force plates can also be used to collect data of a small number of strides [4], however this approach requires expensive force plates which are adequate to measure the ground contact point and contact force for a static simulation, but not for a dynamical approach.

Inertial measurement units (IMUs) using accelerometers and gyroscopes although ideal to capture human are unable to maintain long-term accuracy due to sensor drifting issues [6]. The influence of some other sensors such as camera calibration and markers size on the performance of video-based motion capturing systems was reported in [5].

A new symmetry angle (SA) index has been considered in [10] as a substitute for the symmetry index (SI) in assessing asymmetry. Joint bracing was considered to assess movement differences of limb joints for an asymmetric gate dynamics [11]. Inflated ground reaction forces and symmetry index (SI) values have been reported by Herzog et al. [12] in the assessment of gait asymmetry as a result of dividing a reference average by a very small (close to zero) reference value.

The physical constraints in fast and low speed running have been analyzed in [14] by evaluation of body energy storage and transfer. A musculoskeletal approach of connected links [7] representing different parts of the body evaluated the associated length, mass center position, and moment of inertia using regression equations [31]. Gait assessment due to injury causing one-sided affection has been discussed in [16] by objective measurements of gait

quality and gait function or self-reported function. A combined gait metric (CGAM) that can be regarded as a benchmark to evaluate and differentiate kinematic and kinetic parameters has been presented in [17]. The newly developed CGAM metric successfully distinguish between multiple asymmetry differences at different walking velocities.

A ratio index (RI), as well as a statistical approach has been considered in [9] to assess gait asymmetry. The study [8] discussed the use of various coefficients such as symmetry index (SI), ratio index (RI), SA and GA, and their consistency in assessing gait.

Unstable and stable, asymmetric and symmetric, periodic motions have been observed in [22], and chaotic trajectories have been detected in [23] using a bifurcation analysis of the upper part of the body. A nonlinear time-series analysis was considered in [32] asses dynamic walking. Nonlinear behavior of a walking model has been concluded in [24], and chaotic dynamics of a bipedal model in [25]. The chaotic dynamics observed in [25] could be part of an interdisciplinary research for diagnosing gait pathologies [4].

Actual recommendations for assessing asymmetric and symmetric periodic or chaotic motion have been reinforced in [8] due to missing standards and establish criteria to differentiate between relatively similar or contradictory results. Therefore, new investigations to better assess gait dynamics while overcoming the limitations of previous studies should be considered.

This paper presents the effects of foot injuries on asymmetry and gait dynamics. For this, a wearable sensors system including,

- a foot-mounted pressure sensors that records the ground contact time, contact point and contact force
- a laser pointer (attached to the subject) to project a laser spot in the plane of motion
- a high-speed camera that records the laser spot motion related to dynamics of the human gait in the plane of motion.

have been used.

A nonlinear timeseries analysis, including Poincare map and Lyapunov exponents have been considered for the assessment of the data. The evaluation of key variables in the assessment of gait dynamics - based on a new projective method which considers the axial rotations, translation and in-plane rotation patterns of the gait in the plane of motion - is performed by analyzing the trajectory of the motion in Matlab.

2 Materials and Methods

2.1 Variables to be measured.

Following a review of the literature regarding human gait dynamics a list of key variables to be measured such as ground contact time, contact force, trajectory, and associated devices have been considered [1, 2, 7, 30]. The dynamics have been assessed in the plane of motion with respect to the sagittal plane that divides the human body into right and left sides, taking into account the axial rotations, translation and in-plane rotation patterns of the gait.

2.2 Summary of equipment

Once the variables to be measured have been considered, i.e., ground contact time, contact force, and trajectory, a range of devices have been selected to allow data collection. A brief description of the equipment used, including the manufacturer details. is presented in Table 1.

Table 1
Outline of the equipment including manufacturer name and details of the devices

Description	Manufacturer	Details
Flexiforce WB201 Sensor	Tekscan	Trimmable 3-pin male connector sensor in three force ranges
Wireless Flexi Force WELF 2	Tekskan	Wireless Economical Load & Force Measurement System 2 (WELF™ 2)
Digital JVC GC-PX100 camcorder	JVC	12.8 MP Camcorder - 1080p (record 500 frames per second)
Laser Pointer	GBBG	Light rechargeable Laser 303 pointer
Camera Tripod	Vantage M10	Nest Vantage M10 Video Camera Tripod

Treadmill	PRECOR	TRM885 Treadmill with ITF technology

2.2.1 Laser Sensor Pointer

Since the walking is to be assessed in the plane of motion with respect to the sagittal plane the trajectory of the laser spot is fundamental in the understanding of the dynamics of the system. To address this, the laser pointer (Fig 1c) was attached to the back of the subject (at the intersection of the sagittal and transverse plane as shown in Fig 3) via a special type of clamp collar device attached to the belt.

The laser pointed was firmly clamped the collar as such it can only move with the body. In the initial position (before start walking or running) the laser spot projected by the laser pointer on the ground is located behind the subject on the line defined by the intersection of the sagittal plane and the plane of motion (running belt surface) at a distance of 30 cm from the coronal plane.

The laser pointer - made by hard aluminum withe an anodized black surface treatment - has the working voltage of 3.7V, wavelength of 532nm, range of 500m-1000m, and an adjustable focus and an APC line circuit control. The setup of the displacement sensor, i.e., laser pointer, can be seen in Fig. 3b.

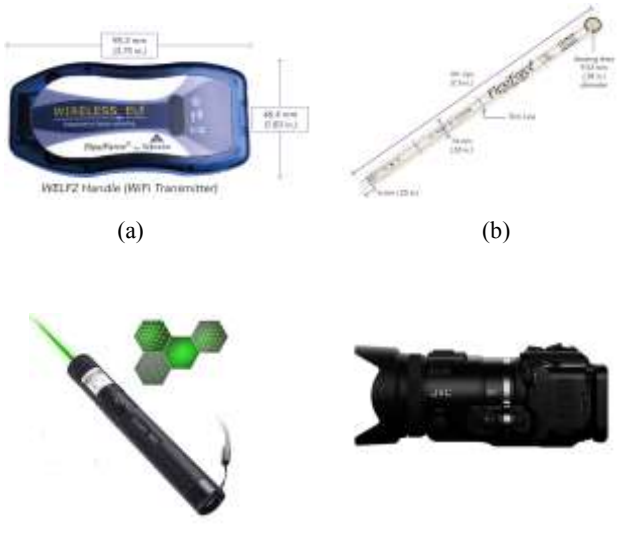

(a) (b)

(c) (d)

Fig. 1. Summary of equipment (a) Wireless Flexi Force WELF 2 handle, (b) Flexiforce WB201 Sensor, (c) Laser sensor (pointer), and (c) Digital camcorder – JVC GC-PX100.

2.2.2 Ground Force Sensor - Flexiforce A201 Sensor

To build up a more accurate image of the gait dynamics device it was necessary to better understand the ground contact point and contact force for a simulated lower leg injury versus a healthy uninjured leg. The lower leg injury was simulated by placing a pebble stone inside the shoe. The dimensions and shape of the pebble stone is shown in Fig. 4. The sensors chosen for this task were piezo-resistive devices of a printed construction from Tekscan, Inc as shown in Fig. 1b. These units are flexible, and are having a thickness of 0.208 mm, a length of 197 mm, a width of 14 mm, and an active sensing area of 9.53 mm diameter. The units made by polyester have 3-pin Male Square Pin (center pin is inactive) connectors with the pin spacing at 2.54 mm. The typical performance as presented in the FlexiForce™ Wireless Economical Load & Force Measurement 2 (WELF™ 2) datasheet has the linearity < ±3% of full scale, repeatability < ±2.5%, hysteresis < 4.5% of full scale, and drift < 5% per logarithmic time scale. The force sensor has been inserted between the insoles and the foam of the trainer sole, thus protecting the sensors from direct contact with the ground.

Fig. 2. Equipment setup including the Precor TRM885 Treadmill with ITF technology, Star 75 Camera Tripod with attached JVC GC-PX100 camcorder.

The Wireless ELF 2 system comes with three WB201 FlexiForce sensors (one in each of the three

available force ranges), that is, WB201-L: Low (0-25 lb; 111 N), WB201-M: Medium (0-150 lb; 667 N), and WB201-H: High (0-1000 lb; 4450 N). For this study the WB201-H sensor was used, i.e., it was inserted inside the running trainer between the insoles and the foam of the trainer sol and connected to the battery-operated WiFi transmitter shown in Fig 1a.

2.2.3 Battery operated WiFi transmitter

To capture the data being generated by the sensor, a Tekscan Wireless ELF 2 handle (Fig 1a) operating under Windows system was considered. The device is capable of transmitting data at two selected frequencies, a low 200 Hz frequency transmitting data at maximum 65 m distance named WELF 2 - basic system, and a high 6000 Hz frequency transmitting data at maximum 25 m distance named WELF 2 - High Speed system. The WELF 2 – basic system could support up to 16 transmitters for a maximum distance of 50 m, while the WELF 2 - High Speed system could support up to 8 transmitters for a maximum distance of 25 m.

The Tekscan Wireless ELF 2 device (Fig 1a) having the dimensions 46.4mm x 26.7mm x 95.3mm, is small and lightweight enough (95 grams) to be placed above the ankle. The device contains its own batteries (3 AAA alkaline batteries) and can be in operation for up to 3 hours at the selected frequency. To ensure repeatability the state of charge i.e., output voltage, of the batteries has been checked at the start of each test.

2.3 Equipment setup

The equipment was set up in a simple way that can be easily replicated. A picture of the setup including the Precor TRM885 Treadmill with ITF technology, the Star 75 Camera Tripod, and the JVC GC-PX100 camcorder is shown in Fig. 1. The tripod/camcorder was placed at 3 m from the end of the treadmill, and the orientation of the camera was 40 degrees with the vertical direction as shown in Fig. 1.

All of the attached equipment i.e., force sensor (Fig 1b), battery operated WiFi transmitter (Fig 1a), and laser pointer (Fig 1c and Fig 3b) was fitted in a non-invasive manner not to affect or significantly influence the use of the foot and the recording of the data, i.e., the trajectory of the laser spot on the treadmill running belt surface (Fig 3a). The total mass of the sensor system, i.e., force sensor and battery-operated WiFi transmitter, attached to the foot was found to be 148 grams.

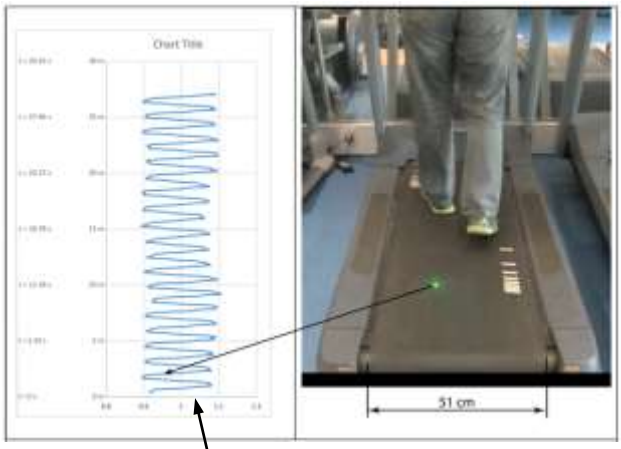

(a)

(b)

Fig. 3. (a) Recorded trajectory of the laser spot for a 30 second time period (approximately 20 – 27 strides) for the gait at 2 mp, (b) Participant walking on a treadmill having the laser pointer attached

2.4 System Testing

Following The system was tested with a healthy individual - a 52-year-old male with a height of 1.80 m and a mass of 97 kg - who did not suffer from any pathology that might adversely affect running style or repeatability. The selection of the participant and testing was conducted following the Bournemouth University ethical approval including the use of Participant Agreement Form and Participant

Information Sheet provided in advance to the participants.
The study required walking/running at 3 different speeds on a Precor TRM885 Treadmill in order to in order to assess some key variables such as the foot ground reaction force and trajectory of motion. A laser sensor (pointer) was attached to a belt around the participant waist (Fig 4.) and the spot of the laser pointer was projected on the treadmill running belt (Fig 3 and Fig 4). The study consisted in recording data related to dynamics of the participant (trajectory of the laser spot) captured in the plane of motion (on the treadmill running belt). The session lasted approximately 60 minutes.

Fig. 4. Pebble stone used to simulate a lower leg injury

The participant was informed about the devices to be used and questioned if the walking and running on the treadmill was comfortable. He was allowed 15 to 30 minutes to warm up by choosing his own pace and cadence at which he felt most comfortable and get used to the device to ensure that the setup and the additional mass of the instrumentation would not cause any issues. Healthy participants have been considered for this preliminary study, while disable individuals (lower limb amputees) will be considered in further studies.

3 Results

The investigation of chaotic behaviour in medical science and engineering represents essential aspects of research emphasizing the effect and significance of chaos (random and unpredictable behaviour in systems in which "uncertainties increase at an exponential rate") within these disciplines [32]. There are various techniques to determine chaos in dynamical systems related to biology and medicine. Some of the most well-known techniques namely phase space analysis, power spectrum, trajectory tracing or bifurcation diagram are qualitative analysis approaches requiring the interpretation of the results. On the other side, the Lyapunov exponents technique is a quantitative analysis approach offering some significant advantages over the previous mentioned techniques. To name some, Lyapunov exponents can

a) be computed from time series obtained from experimental data
b) reveal the stability of a system
c) identify the existence of chaos
c) indicate the exponential separation of nearby trajectories
f) be robust to noise, change in data, and increase of sample size
In this section, the dynamic evolution of the system is investigated using the Lyapunov exponents method.
Data from an exercise trial on a treadmill has been collected for normal human gait (healthy individual) and simulated gait pathology, i.e., healthy individual with a simulated leg injury. The data represents the trajectory of the laser sensor recorded for a 30 second time period (approximately 20 – 29 strides) for the gait at 2 mph, 4 mph and 6 mph as shown in Fig. 3.
The trajectory of the laser spot displacement gathered for the gait at 2 mph for a healthy individual and for a healthy individual with a simulated injury is shown in Fig 5.

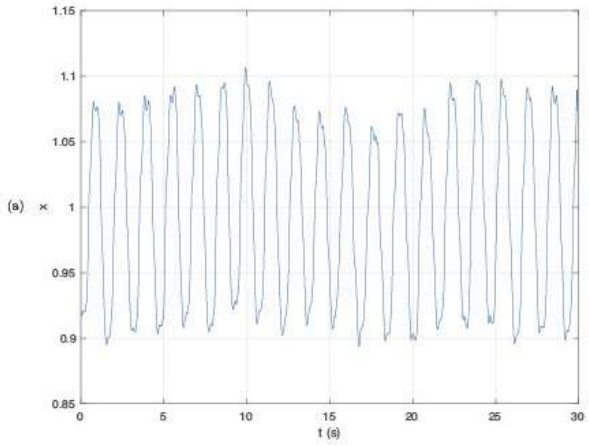

(a)

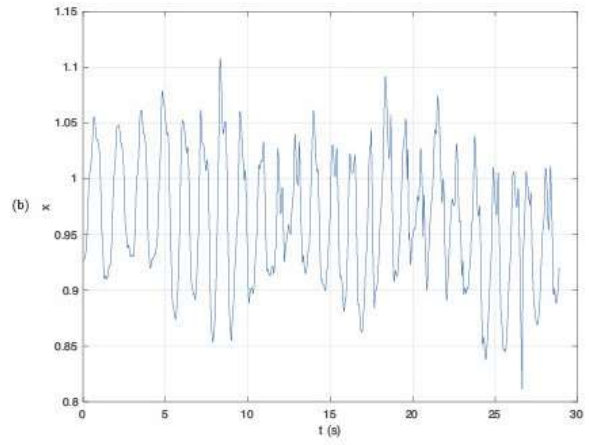

(b)

Fig. 5. Trajectory of the laser spot gathered for the gait at 2 mph for, a) healthy individual, and, b) healthy individual with a simulated injury.

Figure 6a shows the phase plane portrait for the laser spot displacement data gathered for the gait at 2 mph for a healthy individual while Fig. 6a shows the phase plane portrait for the laser spot displacement data for the same healthy individual with the lower leg simulated injury. The trajectory shown in Fig. 6 is associated with the motion around the attractor and shows the classical characteristics of nonperiodic motion [19]. It is visible in both cases that the phase trajectory does not close due to the nonlinearities in the system, that is, the system exhibits a complex dynamic such as chaos as seen in Figs. 6a and Fig. 6b.

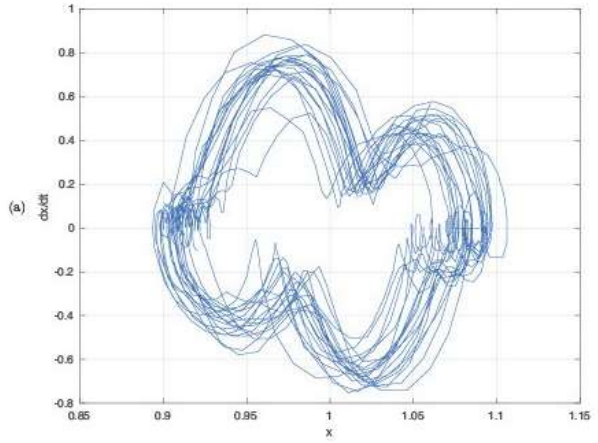

(a)

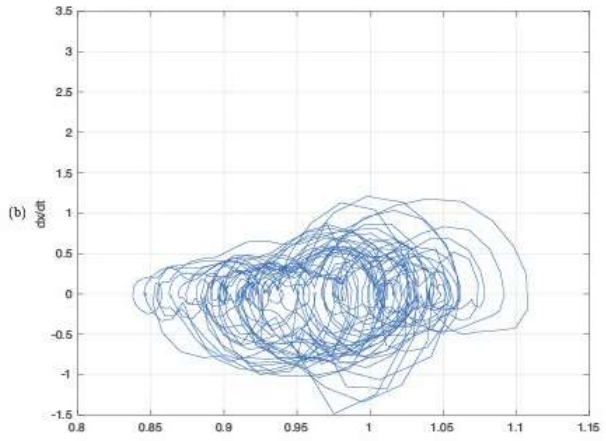

(b)

Fig. 6. Dynamical trajectories of the system in the phase plane for a) healthy individual, and b) healthy individual with a simulated injury

From Fig. 6 it can be seen that the dynamical trajectory of the system does not converge with the increase in the number of interactions, while the associated trajectory of the simulated injury in phase plane resembles mostly a nonperiodic wobbly curve. The return map of the maxima (Poincare map) viewed as the cross section of the trajectory in state space provide an enhanced perspective of the system periodicity [20].

Since a Poincare map detects the intersection points of the trajectory for a specific section when the intersection points of the previous section are known, i.e., describe how the points of a section get mapped back onto the section, the result helps to identify the type of the attractor.

A finite set of points with the number of points corresponding to the period of the attractor define a periodic attractor, while a Poincare map with a closed orbit define a quasiperiodic motion. For the Poincare maps shown in Figure 7a and 7b the data is not periodic or quasiperiodic. The Poincare map of a chaotic attractor appears as a large/infinite number of randomly grouped and respectively ungrouped scatter dots, that is, the case in Fig. 7a and Fig. 7b.

To assess the walking/running variations in the gait pattern i.e., the trajectory of the human gait captured in the plane of motion, the state space of the attractor was reconstructed using time delays and nonlinear dynamics embedding dimension techniques [21]. The purpose of the delays embedding method was to unfold the state space projection of the observed gait trajectory back to the state space that represents the system.

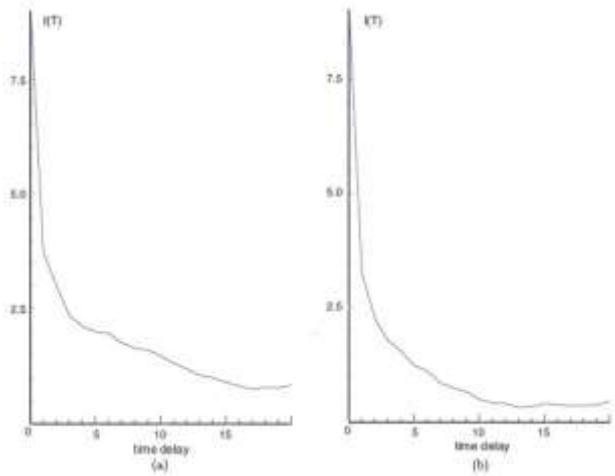

Fig. 7. The Poincare map. The dots dispersion indicates a chaotic and respectively a hyperchaotic time series.

For the reconstruction of the phase space, the time delay used as important information to certify that the delayed coordinates are not dependent on the initial data and the dynamical properties of the original system are preserved, is calculated as depicted in Fig. 8.

The method of delay [21] was used to reconstruct the state space $X(t)$ from the time series by

$$X(t) = [x(t), x(t + \mathrm{T}), x(t + 2\mathrm{T}), \dots, \mathrm{x}(t + m)\mathrm{T})]$$

A proper time delay T is selected at first local minimum connecting the delayed time series and the original data, that is the average mutual information calculated for various time delays based on an iterative process [21].

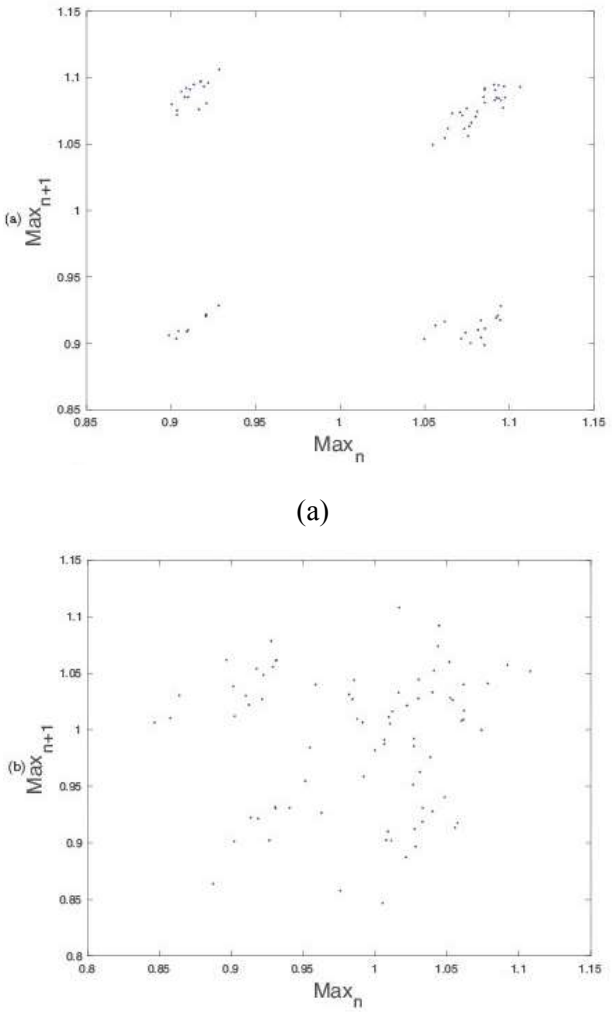

Fig. 8. The initial minimum average mutual information for a) healty individual data is located at the time delay *T*=17, and for b) healty individual with a simulated injury data is located at the time delay *T*=13

The time delay determined by the difference between the actual and the delayed state of the system using the average mutual information as a function of time [26] is shown in Fig. 8. The time delay calculated for the trial in Fig. 8a, i.e., healty individual, is T=17, and for an helathy individual with a simulated injury (Fig. 8b) is T=13.

The proper embedding dimension of the time series is determined from the false nearest neighbours (FNN) method by calculating the distance between neighbouring points in order to unfold the reconstructed walking/running attractor in a suitable state space.

The FFN percentage was calculated at the highest embedding dimension defined by number of independent variables, until the dimension reached a zero percent FFN [27]. From Fig. 9 it can be seen that the total FFN percentage declines and dE is chosen where this percentage approaches zero, that is, the embedding dimension d_E=3.

Selecting a minimum embedding dimension have been considered a key element for decreasing the noise associated the dynamical system.

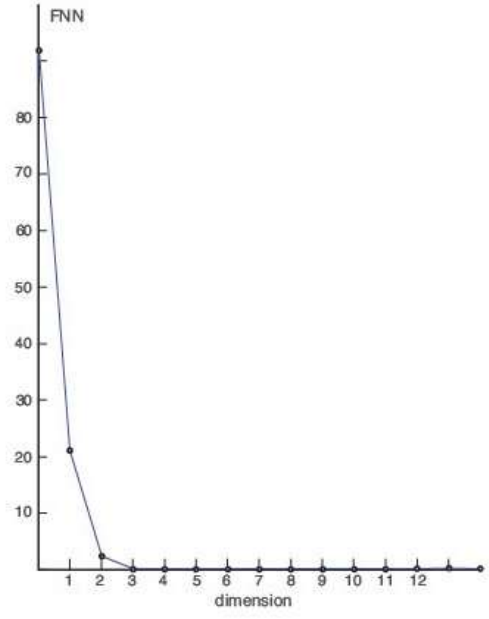

Fig. 9. The percentage of false nearest neighbours against the time series in Fig. 8a for the healthy individual data located at the time delay *T*=17 shows that d_E=3.

The Lyapunov exponents which quantity the degree of separation of nearby trajectories are used to distinguish between the chaotic and non-chaotic behaviour in the state space, determine the nonlinear structure of the attractor, and analyze the local stability of the system [18,26].

The type of dynamical evolution of the system is best shown by the sign of the Lyapunov exponents [13], one positive exponent indicates and chaotic motion, more than one positive exponent indicate instability and hyperchaotic behavior, while negative or zero exponents indicate a periodic motion.

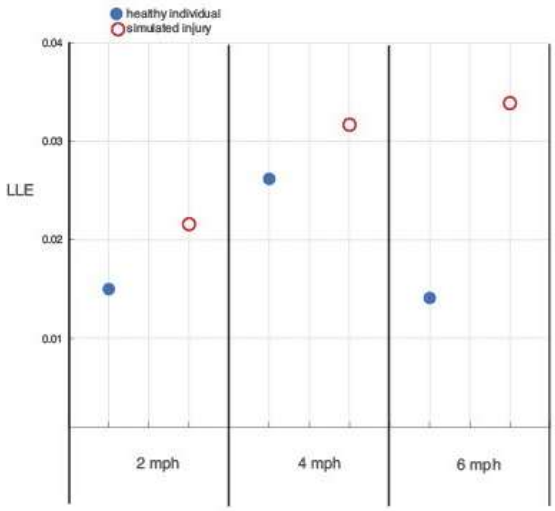

Fig. 10. Largest Lyapunov exponents calculation for the gait at 2 mph for (a) healthy individual (blue plain circular dots), and (b) same healthy individual with a simulated injury (red empty circular dots)

To determine the sign of Lyapunov exponents and to characterize the behavior of the system the computation method developed in [15,21] was used. The divergence of nearest neighbors in state space [21] is estimated as

$$d_j(i) = C_j e^{\lambda(i\Delta t)}$$

where λ is the largest Lyapunov exponent estimated as

$$y(i) = \frac{\langle \ln(d_j(i)) \rangle}{\Delta t}$$

with $\langle . \rangle$ representing the average over j.

Fig. 10 shows the values of the largest Lyapunov exponents calculated for the laser spot trajectory gathered for the gait at 2 mph, 4 mph, and 6 mph for the healthy individual (blue plain circular dots) and for the same healthy individual with a simulated injury (red empty circular dots).

The value of the largest Lyapunov exponent quantifies the exponential divergence of the neighboring trajectories in the reconstructed state space and reflects the degree of chaos in the system. The sign of the largest Lyapunov exponents is positive for all data denoting the exponential separation of nearby trajectories as time evolves, that is, the system is characterized by chaotic behavior. So, one can conclude at this point the chaotic behavior of each system.

The vertical ground reaction force is also an important factor in analyzing and understanding gait dynamics. The ground reaction force data from a treadmill trial has been collected for the healthy individual walking at 2 mph, 4 mph, and 6 mph.

With respect to the magnitude of the vertical ground reaction similar conclusions to the one presented in [29] have been obtained, that is "that stride frequency, stride length and contact length" increased at higher speed by applying greater forces to the ground. The conclusion is also in good agreement with the one obtained in [28] showing a linear increase in ground force from 1.2 body weight (BW) during walking to approximately 2.5 BW when running at 6.0 m/s.

4 Conclusion

This study provides new information about the effect of foot injury on gait dynamics. The approach was based on a new projective method which considers the axial rotations, translation and in-plane rotation patterns of the gait in the plane of motion. Poincare map, phase space, FNN method, Lyapunov exponents and correlation dimension – which offer excellent quantifications for various characteristics of gait dynamics - have been considered to validate the assessment. The positive sign of the largest Lyapunov exponents for all data indicate "the exponential separation of nearby trajectories with time", that is, the chaotic behavior of the system.

Acknowledgement:
This research was conducted at the facilities of the Department of Design and Engineering, Bournemouth University.

Source of Funding:

The research was funded by the Department of Design and Engineering, Faculty of Science and Technology, Bournemouth University.

Conflict of interest:
The authors have no conflicts of interest to declare that are relevant to the content of this article.

Contribution of Individual Authors to the Creation of a Scientific Article:
Mihai Dupac, has organized and executed the experiment presented in Section 2.
Dan B. Marghitu carried out the simulation presented in Section 3.
Both authors discussed the results and contributed to the final version of the manuscript.

References:
[1] Liu T., Inoue Y., Shibata K. (2009). Development of a wearable sensor system for quantitative gait analysis. Measurement, 42, 978-988.
[2] Sardini E., Serpelloni M., Lancini M. (2015). Wireless Instrumented Crutches for Force and Movement Measurements for Gait Monitoring, IEEE Transactions on Instrumentation and Measurement, 64(12), 3369-3379.
[3] Palermo E., Rossi S., Marini F., Patane F., Cappa P. (2014). Experimental evaluation of accuracy and repeatability of a novel body-to-sensor calibration procedure for inertial sensor-based gait analysis. Measurement, 52, 145-155.
[4] Hunter J., Marshall R., McNair P. (2005). Relationships between ground reaction force impulse and kinematics of sprint-running acceleration. Journal of applied biomechanics, 21(1), 31–43.
[5] Windolf M., Götzen N., Morlock M. (2008). Systematic accuracy and precision analysis of video motion capturing systems—exemplified on the Vicon-460 system. Journal of Biomechanics, 4(12), 2776-2780.
[6] Rebula, J., Ojeda, L., Adamczyk, P., Kuo, A. (2013). Measurement of foot placement and its variability with inertial sensors. Gait & Posture, 38, 974–980.
[7] Dorschky E., Nitschke M., Seifer A.-K., van den Bogert A. J., Eskofier B. M., (2019). Estimation of gait kinematics and kinetics from inertial sensor data using optimal control of musculoskeletal models, Journal of Biomechanics, 95, 1-9, 109278.
[8] Błażkiewicz M., Wiszomirska I., Wit A., (2014). Comparison of four methods of calculating the symmetry of spatial-temporal parameters of gait, Acta of Bioengineering and Biomechanics, 16 (1), 29-35
[9] Sadeghi H., (2003). Local or global asymmetry in gait of people without impairments, Gait & Posture, 17 (3), 197–204.
[10] Zifchock R., Davis I., (2008). The symmetry angle: A novel, robust method of quantifying asymmetry, Gait & Posture, 27 (4), 622–627
[11] Shorter K., Polk J., Rosengren K., Hsiao-Wecksler E., (2008). A new approach to detecting asymmetries in gait, Clinical Biomechanics, 23 (4), 459–467
[12] Herzog W., Nigg B., Read L., Olsson E., (1989) Asymmetries in ground reaction force patterns in normal human gait, Med. Sci. Sports Exerc., 21 (1), 110–114
[13] Wolf A., Swift J.B., Swinney H.L., Vastano J.A., (1985). Determining Lyapunov exponents from a time series, Physica D: Nonlinear Phenomena, 16 (3), 285-317.
[14] Cavagna G.A., (2010). Symmetry and Asymmetry in Bouncing Gaits, Symmetry, 2, 1270-1321
[15] Rosenstein M.T., Collins J.J., De Luca C.J., (1993). A practical method for calculating largest Lyapunov exponents from small data sets, Physica D: Nonlinear Phenomena, 65 (1–2), 117-134.
[16] Hodt-Billington C., (2012) Measures of symmetry in gait: Methodological principles and clinical choices, Dissertation for the degree philosophiae doctor (PhD) at the University of Bergen.
[17] Ramakrishnan T., Lahiff C.-A., Reed K.B., (2018). Comparing Gait with Multiple Physical Asymmetries Using Consolidated Metrics, Front. Neurorobot., 12 (2), 1-12
[18] Kantz H., Schreiber T., (2003). Nonlinear time series analysis, Cambridge University Press, 2nd Edition.
[19] Liu X., Vlajic N., Long X., Meng G., Balachandran B., (2013). Nonlinear motions of a flexible rotor with a drill bit: stick-slip and delay effects. Nonlinear Dynamics, 72 (1), 61–77.
[20] Strogatz, S.H., (2018). Nonlinear Dynamics and Chaos: with Applications to Physics, Biology, Chemistry, and Engineering, CRC Press
[21] Zhao J., Marghitu D.B., (2020). Scumacher J., Tranquilizer effect on the Lyapunov exponents of lame horses, Helyon, 6, e03726
[22] Luo A.C.J., Huang J., (2013). Asymmetric periodic motions with chaos in a softening

duffing oscillator, International Journal of Bifurcation and Chaos, 23, (05), 1350086.
[23] Borzova E., Hurmuzlu Y., (2004). Passively walking five-link robot, Automatica 40, 621–629
[24] Wisse M., Schwab A.L., Van Der Helm F.C.T., (2004). Passive dynamic walking model with upper body, Robotica, 22, 681–688.
[25] Kurz M.J., Stergiou N., Heidel J., Foster E.T., (2005). A template for the exploration of chaotic locomotive patterns, Chaos Solitons Fractals, 23, 485–493
[26] Abarbanel H.D.I., (1996). Analysis of Observed Chaotic Data. Springer, New York.
[27] Fraser A.M., Swinney H.L., (1986). Independent coordinates for strange attractors from mutual information, Phys. Rev. A, 33, 1134.
[28] Keller T.S., Weisberger A.M., Ray J.L., Hasan S.S., Shiavi R.G., Spengler D.M., (1996). Relationship between vertical ground reaction force and speed during walking, slow jogging, and running. Clinical Biomechanics, 11 (5), 253-259
[29] Weyand P.G., Sternlight D.B., Bellizzi M.J., Wright S., (2000). Faster top running speeds are achieved with greater ground forces not more rapid leg movements. Journal of Applied Physiology, 89 (5), 1991-1999
[30] Hawkins J., Noroozi S., Dupac M., Sewell P., (2016). Development of a wearable sensor system for dynamically mapping the behavior of an energy storing and returning prosthetic foot, Measurement Science Review, 16 (3), 174-182
[31] Winter, D. A., (2009). Biomechanics and motor control of human movement, John Wiley & Sons.
[32] Sajid Iqbal, (2016). Research on chaos in passive dynamic walking using nonlinear time-series analysis, Dissertation for the Doctoral Degree in Engineering, School of Mechatronics Engineering, Harbin Institute of Technology

Contribution of Individual Authors to the Creation of a Scientific Article (Ghostwriting Policy)

The authors equally contributed in the present research, at all stages from the formulation of the problem to the final findings and solution.

Sources of Funding for Research Presented in a Scientific Article or Scientific Article Itself

No funding was received for conducting this study.

Conflict of Interest

The authors have no conflicts of interest to declare that are relevant to the content of this article.